

## Synaptic Depression Leads to Nonmonotonic Frequency Dependence in the Coincidence Detector

**Shawn Mikula**

*mikula@jhmi.edu*

**Ernst Niebur**

*niebur@jhu.edu*

*Krieger Mind/Brain Institute and Department of Neuroscience,  
Johns Hopkins University, Baltimore, MD 21218, U.S.A.*

In this letter, we extend our previous analytical results (Mikula & Niebur, 2003) for the coincidence detector by taking into account probabilistic frequency-dependent synaptic depression. We present a solution for the steady-state output rate of an ideal coincidence detector receiving an arbitrary number of input spike trains with identical binomial count distributions (which includes Poisson statistics as a special case) and identical arbitrary pairwise cross-correlations, from zero correlation (independent processes) to perfect correlation (identical processes). Synapses vary their efficacy probabilistically according to the observed depression mechanisms. Our results show that synaptic depression, if made sufficiently strong, will result in an inverted U-shaped curve for the output rate of a coincidence detector as a function of input rate. This leads to the counterintuitive prediction that higher presynaptic (input) rates may lead to lower postsynaptic (output) rates where the output rate may fall faster than the inverse of the input rate.

### 1 Introduction

---

Neuronal populations frequently employ mean firing rate to encode information about stimulus features. To encode information about either internal states of the observer or derived properties of the stimulus, such as saliency, expectancy, or feature binding, both models and experimental evidence suggest that neural synchrony or cross-correlation is used in addition (Niebur & Koch, 1994; Decharms & Merzenich, 1996; König, Engel, & Singer, 1996; Alonso, Usrey, & Reid, 1996; Gray & Viana Di Prisco, 1997; Fries, Roelfsema, Engel, König, & Singer, 1997; de Oliveira, Thiele, & Hoffmann, 1997; Riehle, Grün, Diesmann, & Aertsen, 1997; Roelfsema & Singer, 1998; Steinmetz et al., 2000; Salinas & Sejnowski, 2001; Niebur, 2002; Niebur, Hsiao, & Johnson, 2002). Thus, neural responses have to be understood as a function of both the presynaptic mean rate and the correlation structure of synaptic inputs.

Using combinatorial methods, we have previously found the analytical solution for the output rate of an ideal coincidence detector that receives an arbitrary number of input spike trains with identical binomial count distributions (which includes Poisson statistics as a special case) and identical pairwise cross-correlations (Mikula & Niebur, 2003). In that solution, synaptic strength was assumed to be constant. In this article, we extend our previous results to include the practically important case of frequency-dependent synaptic depression.

Many synapses, mainly between pyramidal cells in cortex and related systems, show strong synaptic depression. This means that the postsynaptic effect of a synapse is largest for the first incoming action potential, becomes successively smaller for subsequent spikes, and recovers gradually in the absence of further synaptic input (Thomson & Deuchars, 1994; Varela et al., 1997; Markram & Tsodyks, 1996; Nelson & Smetters, 1993; Finnerty, Roberts, & Connors, 1999; Matveev & Wang, 2000). Synaptic depression has been proposed to underlie numerous mechanisms, including cortical gain control (Abbott, Varela, Sen, & Nelson, 1997), removal of the dependence of mean firing rate on transient rate changes (Abbott et al., 1997), contrast independence and adaptation in V1 simple cells (Chance, Nelson, & Abbott, 1998), redundancy reduction in spike trains (Goldman, Maldonado, & Abbott, 2002), generation of neural synchrony (Loebel & Tsodyks, 2002), and generation of direction-selective responses in V1 (Buchs & Senn, 2002).

Experimental studies of synaptic depression typically determine the average amplitude of excitatory postsynaptic potentials (EPSPs). Changes in the mean amplitude can be due to changes in the amplitude of each individual EPSP, without changing the total number of EPSP, and changes in the number of individual EPSPs, without changing the amplitude of individual EPSPs. We focus on the latter and refer to it as *probabilistic* synaptic depression (also called *stochastic* synaptic depression by Goldman et al., 2002). Thus, we assume that the probability of an EPSP varies, while the amplitude of each EPSP is constant. We study this case because the amplitudes of EPSPs of many synapses in cortex and hippocampus take on only one value (or a few discrete values) while the probability of generating an EPSP may vary over a continuum (for a review, see Korn & Faber, 1991; Walmsley, Alvarez, & Fyffe, 1998).

Previous theoretical work (Abbott et al., 1997; Senn, Segev, & Tsodyks, 1998) has focused on the influence of synaptic depression on neural responses to presynaptic transients, having the most drastic effects when the presynaptic firing rates change abruptly. In this article, we study the complementary case of a steady-state situation, assuming long spike trains with constant rates, and we obtain an analytical solution for the output rate of the coincidence detector. Perhaps counterintuitively, it is found that for a large part of the parameter space, the output rate decreases (rather than reaching an asymptote) for increasing input rate. Thus, it is found that synaptic depression, if made sufficiently strong, will result in nonmonotonic depen-

dence of the output rate of a coincidence detector as a function of input rate.

## 2 Methods

---

**2.1 Model Neurons: Coincidence Detectors.** The type of model neurons used in this study are coincidence detectors. Coincidence detectors are computational units that fire at time  $t$  if the number of unit EPSPs received within the window  $(t - T, t)$  equals or exceeds the threshold  $\theta$ . Without limiting generality, we chose  $T = 10$  ms. This is the timescale of fast synaptic conductances, and it is at this timescale that synaptic events superpose and interact.

**2.2 Binomial Spike Trains with Specific Cross-Correlation.** Previously, we introduced a systematic method for the generation of an arbitrary number of spike trains with specified pair-wise mean cross-correlations and firing rates (Mikula & Niebur, 2003). Action potentials are distributed according to binomial counting statistics in each spike train. Mean firing rates and cross-correlations are the same for all spike trains (or all pairs of spike trains, respectively), but they can be chosen independently of each other. We describe the procedure here for the convenience of the reader.

Let  $m$  be the number of input spike trains, each having  $n$  time bins. All bins are of equal length  $\delta t$ , chosen sufficiently small so that each contains a maximum of one spike; that is, each bin is guaranteed to contain either one or zero spikes. The coincidence detector makes the decision whether to fire within one time bin; therefore,  $T = \delta t$ . Assuming a firing rate of

$$f = \frac{p}{\delta t}, \quad (2.1)$$

the probability that a spike is found in any given time bin is  $p$ ; no spike is found with probability  $(1 - p)$ . Bins in any given spike train are independent, which implies that the following analysis can be limited to a single time bin. Note that the physiologically important Poisson statistics are the special case of low rates and long spike trains.

A specific correlation coefficient  $q$  (with  $0 \leq q \leq 1$ ) between any two spike trains is introduced by first generating  $m + 1$  independent spike trains with mean firing rates  $f$ . We designate spike train number  $m + 1$  as the reference spike train. In order to introduce the correlation coefficient  $q$  between spike trains  $1, = 2, \dots, m$ , we switch, with a probability  $\sqrt{q}$ , the state (one or zero spikes) of a time bin in each of these spike trains to that found in the reference spike train. This yields a mean correlation coefficient of  $q$  between any two of the spike trains  $1, \dots, m$  while maintaining the mean firing rate as  $p/\delta t$ . In the appendix, it is shown that  $q$  is the usual Pearson correlation coefficient.

**2.3 Synaptic Depression.** With the intent of constructing a realistic model of synaptic depression, we begin with the following equation, slight variations of which have been derived by previous investigators (Tsodyks & Markram, 1997, from where we take part of our notation):

$$\langle EPSP_{n+1} \rangle = \langle EPSP_n \rangle \cdot (1 - U_{se}) \cdot e^{-\Delta t/\tau_d} + A \cdot (1 - e^{-\Delta t/\tau_d}), \quad (2.2)$$

where  $\langle EPSP_n \rangle$  is the mean amplitude of the  $n$ th EPSP with the average taken over trials,  $\tau_d$  is the recovery time constant for the synaptic depression,  $\Delta t$  is the time interval between the  $n$ th and  $(n+1)$ st input spike,  $U_{se}$  is the fraction of presynaptic resources used in response to a presynaptic spike, and  $A$  is the average EPSP generated in the limit as the input spike frequency approaches zero. The experimental range of  $U_{se}$  and  $\tau_d$  is 0.1 to 0.95 and 500 to 1500 ms, respectively (Markram, 1997). The interspike interval  $\Delta t$  is, in general, a function of  $n$ , but we suppress the argument to alleviate the notation.

Note that equation 2.2 does not specify the microscopic mechanism by which the average amplitude  $\langle EPSP_n \rangle$  is modified by the depression mechanism. The mechanism could be a decrease in either the amplitude of individual synaptic events or the probability of generating an EPSP of constant amplitude, or any combination of these two.

Neurotransmitter is stored in vesicles and released in discrete (quantal) units (Del Castillo & Katz, 1954). The amplitude of an EPSP (seen as either a conductance change of the postsynaptic membrane, a current injected into the postsynaptic cell, or a voltage change across the postsynaptic membrane) is the sum of the postsynaptic effects of these quanta. As long as the number of quantal releases per event is large, it may be possible to approximate this sum by a continuous variable, the mean EPSP amplitude  $\langle EPSP_{n+1} \rangle$  in equation 2.2. This is not appropriate, however, for modeling synaptic events in which only one release site exists at the synapse or only one quantum of neurotransmitter may be released from the release site per presynaptic spike, as has been found in many cases (Schikorski & Stevens, 1997; Silver, Cull-Candy, & Takahashi, 1996; Stevens & Wang, 1995; Arancio, Korn, Gulyas, Freund, & Miles, 1994; Gulyas et al., 1993). EPSPs at such synapses are all-or-nothing events that can only assume either some nonzero positive value (when one quantum is released) or zero (when no quantum is released). Similar considerations apply if the postsynaptic mechanisms are quantized with a small number of quanta per synaptic event and for mechanisms that discretize the size of the synaptic events, such as postsynaptic saturation (Tong & Jahr, 1994; Auger, Kondo, & Marty, 1998).

For synapses whose postsynaptic events consist of a small number of events (unit EPSPs), equation 2.2 may be reinterpreted as governing the probability  $P(EPSP_{n+1})$  for a unit  $EPSP_{n+1}$  to occur:

$$P(EPSP_{n+1}) = P(EPSP_n) \cdot (1 - U_{se}) \cdot e^{-\Delta t/\tau_d} + A \cdot (1 - e^{-\Delta t/\tau_d}), \quad (2.3)$$

where  $A$  is now the average probability in the limit as  $\Delta t \rightarrow \infty$ . Equation 2.3 produces a depression in the probability that a unit EPSP will be induced, by either decreasing synaptic vesicle release probability from a single synaptic release site, or by lowering the probability that the presynaptic release will be registered by the postsynaptic membrane.

Experimental evidence suggests that synapses modeled by equation 2.3 are predominant between pyramidal cells in cortex and hippocampus. The condition that there exists only one or very few release sites per synapse has both ultrastructural (Schikorski & Stevens, 1997) and neurophysiological (Auger & Marty, 1997; Silver et al., 1996; Arancio et al., 1994; Gulyas et al., 1993; Raastad, Storm, & Andersen, 1992) support, though evidence to the contrary does exist (Hornoch, Martin, Jack, & Stratford, 1998).

### 3 Results

---

**3.1 Constant Synaptic Strength.** An analytical solution of a coincidence detector receiving input of the type introduced in section 2.2 was reported in our previous work (Mikula & Niebur, 2003). It is difficult, however, to take synaptic depression into account in the solution presented there because it is obtained in terms of the initial number of coincident spikes, prior to applying the cross-correlation procedure.

We now introduce an alternative analytical derivation of  $P_{out}(p, m, \theta, q)$ , the probability that the coincidence detector produces an output spike (in this time bin) when it receives  $m$  input spike trains with cross-correlation  $q$ . This derivation, though similar in spirit to that presented by Mikula and Niebur (2003), differs in that we obtain an equation for  $P_{out}(p, m, \theta, q)$  as a summation over the final number of coincident spikes rather than over the number of coincident spikes before introducing correlations. This alternative formulation is more suitable for the subsequent incorporation of probabilistic synaptic depression and is presented in the following section.

Consider the following expression:

$$P_{out}(p, m, \theta, q) = \sum_{i=\theta}^m (C_1 + C_2), \quad (3.1)$$

where  $C_1$  and  $C_2$  will be defined in the subsequent paragraph, and the summation is over the number of coincident input spikes after the correlation procedure in section 2.2 has been completed.

The terms  $C_1$  and  $C_2$  are the contributions obtained in the cases of  $j \leq i$  and  $j \geq i$ , respectively.<sup>1</sup> We first compute  $C_1$ . If the initial number of coincident input spikes,  $j$ , is greater than or equal to the final number,  $i$ , then it is only possible to “lose” spikes to obtain exactly  $i$  if there exists

---

<sup>1</sup> It will become clear below why the case  $j = i$  is included in both terms of equation 3.1.

a zero in the reference spike train; this occurs with probability  $1 - p$ . The initial number of coincident input spikes,  $j$ , is binomially distributed, which contributes a factor of  $\binom{m}{j} p^j (1 - p)^{m-j}$ . Since the probability of switching a time bin of an input spike train to the value in the reference train is  $\sqrt{q}$ , the factor representing the probability for  $i$  of the  $j$  initially coincident input spikes not to switch to the value of the reference, which is zero for this case, is given by the binomial distribution as  $\binom{j}{i} \sqrt{q}^{j-i} (1 - \sqrt{q})^i$ . Having computed all the relevant factors, the joint probability  $C_1$  is obtained as the product of the already noted factors,

$$C_1 = \sum_{j=i}^m \binom{m}{j} p^j (1 - p)^{m-j} \binom{j}{i} \sqrt{q}^{j-i} (1 - \sqrt{q})^i (1 - p). \quad (3.2)$$

We now derive the joint probability for  $C_2$ , representing the case where  $j$ , the initial number of coincident input spikes, is less than or equal to the final number  $i$ . The only way to “gain” spikes to obtain exactly  $i$  is if there exists a spike in the reference; this occurs with probability  $p$ . As in the derivation for  $C_1$ , we consider that the initial number of coincident input spikes,  $j$ , is binomially distributed, which adds a factor of  $\binom{m}{j} p^j (1 - p)^{m-j}$ . Since the probability of switching a time bin of an input spike train to the value in the reference train is  $\sqrt{q}$ , the factor representing the probability for  $i - j$  of the  $m - j$  initially coincident input nonspikes to switch to the value of the reference, which is one for this case, is given by the binomial distribution as  $\binom{m-j}{i-j} \sqrt{q}^{i-j} (1 - \sqrt{q})^{m-i}$ . The joint probability  $C_2$  is then the product,

$$C_2 = \sum_{j=0}^i \binom{m}{j} p^j (1 - p)^{m-j} \binom{m-j}{i-j} \sqrt{q}^{i-j} (1 - \sqrt{q})^{m-i} p. \quad (3.3)$$

As already noted, the case  $i = j$  is contained in both equations 3.2 and 3.3. In equation 3.2,  $C_1$  combines all cases in which the original spike train (before applying the switching procedure) had as many or more spikes than after the switching ( $j \geq i$ ). For  $j > i$ , a spike train with  $j$  spikes can be transformed into one with  $i$  spikes only if the reference spike train has a 0 in this time bin; these are the terms with  $j > i$  in equation 3.2. Likewise, a spike train with  $j < i$  spikes can be transformed into one with  $i$  spikes only if the reference spike train has a 1 in this time bin; these are terms with  $j < i$  in equation 3.3. For  $j = i$ , however, the number of spikes is not changed during the switching, and this can happen with a reference spike train with both a 0 and with a 1. The probability that the number of spikes is not changed is simply the probability that  $i$  spikes are present (which implies  $m - i$  zeroes) and that none of these is switched. This probability is

$$\binom{m}{i} p^i (1 - p)^{m-i} (1 - \sqrt{q})^i, \quad (3.4)$$

and it is seen by direct substitution that this is the sum of the two terms with  $j = i$  in equations 3.2 and 3.3.

Substituting equations 3.2 and 3.3 in equation 3.1, we obtain the following expression:

$$\begin{aligned}
 P_{out}(p, q, m, \theta) &= \sum_{i=\theta}^m \left( \sum_{j=i}^m \binom{m}{j} p^j (1-p)^{m-j} \binom{j}{i} \sqrt{q}^{j-i} (1-\sqrt{q})^i (1-p) \right. \\
 &\quad \left. + \sum_{j=0}^i \binom{m}{j} p^j (1-p)^{m-j} \binom{m-j}{i-j} \sqrt{q}^{i-j} (1-\sqrt{q})^{m-i} p \right). \quad (3.5)
 \end{aligned}$$

We have thus obtained an exact analytical solution for the output rate of a coincidence detector receiving an arbitrary number of inputs with identical binomial statistics and modulated with respect to both mean rate and cross-correlation. This solution is an alternative to the one in Mikula and Niebur (2003). The validity of equation 3.5 is confirmed by simulation (not shown) and by comparison with our previous result (Mikula & Niebur, 2003).

**3.2 Probabilistic Synaptic Depression.** We now proceed to derive an expression for the steady-state value of  $P(EPSP)$  in the presence of synaptic depression. Let us assume that spike input is stationary in time, which means that

$$P(EPSP_n) \approx P(EPSP_{n+1}),$$

or, in other words, that  $\langle \Delta t \rangle$  is independent of  $n$  in equation 2.3. The firing frequency  $f = \langle \Delta t \rangle^{-1}$  is then constant, as is the spike probability (per bin)  $p = f \delta t$ . Equation 2.3 is now solved readily,

$$P(EPSP_n) = \frac{A(1 - e^{-1/(f\tau_d)})}{1 - (1 - U_{se})e^{-1/(f\tau_d)}} =: \gamma_0, \quad (3.6)$$

where we have defined the stationary probability  $P(EPSP_n)$  as  $\gamma_0$ .

We can also derive equation 3.6 by generalizing equation 2.3 to

$$\begin{aligned}
 P(EPSP_{n+z}) &= P(EPSP_n) [(1 - U_{se})e^{1/(f\tau_d)}]^z \\
 &\quad + A(1 - e^{-1/(f\tau_d)}) \sum_{i=1}^{z-1} [(1 - U_{se})e^{1/(f\tau_d)}]^i \quad (3.7)
 \end{aligned}$$

for  $z \in \mathbb{N}^+$ . If we again assume stationary input (i.e.,  $f$  constant), equation 3.6 is obtained in the limit  $z \rightarrow \infty$  by noting that the first term on the right-hand

side of equation 3.7 goes to zero and then evaluating the resulting geometric series.

In order to incorporate probabilistic synaptic depression into equation 3.6, let us recall the meaning of  $\gamma_0$ . In words,  $\gamma_0$ , which is a function of the input rate,  $f = p/\delta t$ , is the probability that an input spike generates an EPSP after applying synaptic depression. The existence of a presynaptic spike and the generation of a postsynaptic event by this spike are two independent events, and the probability of the combined event is the product of the two individual events. The probability that  $k$  coincident input spikes remain after applying synaptic depression to  $i$  coincident input spikes (with  $k \leq i$ ) is binomially distributed,  $\binom{i}{k} \gamma_0^k (1 - \gamma_0)^{i-k}$ . We are interested only in  $k \geq \theta$ , and thus we derive the following extension of equation 3.5 that includes the effects of probabilistic synaptic depression:

$$\begin{aligned}
 P_{out}(p, q, m, \theta, U_{se}, \tau_d) &= \sum_{i=\theta}^m \left( \sum_{j=i}^m \binom{m}{j} p^j (1-p)^{m-j} \binom{j}{i} \sqrt{q}^{j-i} (1-\sqrt{q})^i (1-p) \right. \\
 &\quad \left. + \sum_{j=0}^i \binom{m}{j} p^j (1-p)^{m-j} \binom{m-j}{i-j} \sqrt{q}^{i-j} (1-\sqrt{q})^{m-i} p \right) \\
 &\quad \times \sum_{k=\theta}^i \binom{i}{k} \gamma_0^k (1-\gamma_0)^{i-k}. \tag{3.8}
 \end{aligned}$$

Note that the dependence on  $U_{SE}$  and  $\tau_d$  on the right-hand side of this equation is through  $\gamma_0$ . We use the same symbol,  $P_{out}$ , for the output probability both with synaptic depression, equation 3.8, and without, equation 3.5, to simplify the notation but note that the variables can be distinguished, if needed, by the number of their arguments.

We have thus obtained our main result: the output rate of a coincidence detector receiving an arbitrary number of synaptically depressed inputs with identical binomial statistics and modulated with respect to both mean rate and cross-correlation. The result is subject to the approximation leading to equation 3.6. The validity of equation 3.8 is confirmed by simulation (see Figure 3).

## 4 Examples

---

**4.1 Simple Case.** An illustration of equations 3.5 and 3.8 for a coincidence detector receiving  $m = 2$  synaptically depressed binomial input spike trains and with a threshold  $\theta = 2$  is shown in Figures 1a and 1b, respectively. We will also set  $A = 1$  in all plots. For this case, equations 3.5 and 3.8 take

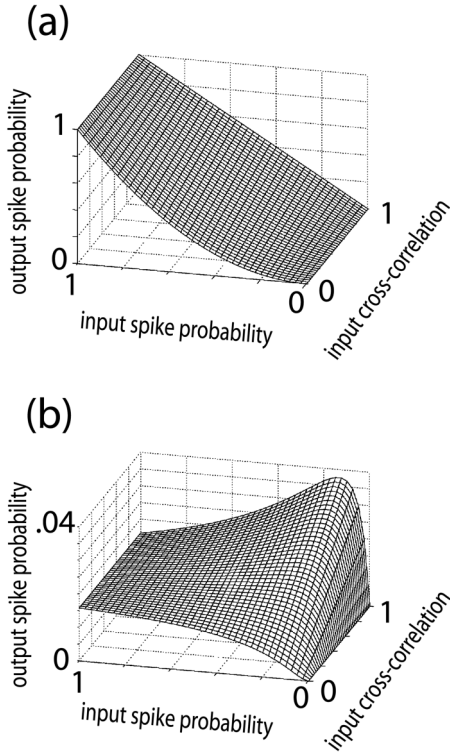


Figure 1: Analytical results for coincidence detector in the simple case. (a) Plot of equation 3.5 (no depression) for  $m = 2$  inputs and threshold of  $\theta = 2$ . (b) Plot of equation 3.8 (with depression;  $m = 2$  inputs,  $\theta = 2$ , synaptic depression parameter values  $U_{se} = 0.1$  and  $\tau_d = 700$  ms).

very simple forms, allowing us to develop an intuition for the solutions that will be useful to retain for more complicated examples.

Let us first consider the case without synaptic depression. We can then use equation 3.5, which reduces to

$$P_{out}(p, q, m = 2, \theta = 2) = p^2(1 - \sqrt{q})^2(1 - p) + \sum_{j=0}^2 \binom{2}{j} p^j (1 - p)^{2-j} \sqrt{q}^{2-j} p. \quad (4.1)$$

We see that for  $q = 0$ , equation 4.1 further reduces to  $P_{out}(p, q = 0, m = 2, \theta = 2) = p^2$ , as expected for independent processes. Likewise, for  $q = 1$ , we obtain  $P_{out}(p, q = 1, m = 2, \theta = 2) = p$ , the result for a single process.

Intermediate correlation values ( $0 < q < 1$ ) interpolate smoothly between these two extremes. In Figure 1a, we produce the surface plot of equation 4.1.

Taking into account synaptic depression, we refer to equation 3.8 and obtain

$$P_{out}(p, q, m = 2, \theta = 2, U_{se}, \tau_d) = \left( p^2(1 - \sqrt{q})^2(1 - p) + \sum_{j=0}^2 \binom{2}{j} p^j (1 - p)^{2-j} \sqrt{q}^{2-j} p \right) \gamma_0^2, \quad (4.2)$$

which is just equation 4.1 multiplied by  $\gamma_0^2$ . Let us gain some insight by considering the limiting cases of very high and very low input frequencies and cross-correlations.

For sufficiently high frequencies, the argument in the exponentials of equation 3.6 is small, and we can develop the exponentials ( $e^{-x} \approx 1 - x$  for  $x \ll 1$ ). We obtain

$$\gamma_0 \approx \frac{A}{U_{se} \tau_d} \cdot \frac{1}{f} \quad (4.3)$$

and see that  $\gamma_0$  is inversely proportional to  $f$  in this approximation. A similar result showing that synaptic depression makes the mean amplitude of EPSPs behave like  $1/f$  was derived by Abbott et al. (1997).<sup>2</sup>

We know from equation 4.3 that  $\gamma_0^2$  is proportional to  $1/f^2$  or, equivalently, to  $1/p^2$ , for frequencies above  $\tau_d^{-1}$ . Based on the argument immediately following equation 4.1, we therefore expect that for zero input cross-correlation, the output of the coincidence detector asymptotically approaches some finite value for increasing input frequencies. For completely cross-correlated inputs, we expect the output to decrease like  $1/p$ . This is exactly what we see in Figure 1b.

For low input rates, the output must increase for increasing input rates (since the output rate is zero for  $p = 0$  and it cannot become negative, the only way is up). For low cross-correlation, we expect that the output frequency monotonically increases with the input frequency, over the whole range from  $p = 0$  to  $p = 1$ , which is what is indeed seen in Figure 1b. Such monotonic behavior is not possible for high cross-correlation since the output rate increases with  $p$  for low  $p$  and decreases as  $1/p$  for high

---

<sup>2</sup> These authors studied the mean amplitude of all EPSPs, which depends on both the probability of generating an EPSP and the mean amplitude of individual EPSPs, as was discussed earlier.

$p$ . This implies that the output rate must peak at some intermediate value of  $p$ , a feature that is again seen in Figure 1b where an optimal mean input rate at an intermediate  $p$  value (where the maximal output rate is observed) is obvious. This is a novel feature not present with nondepressing synapses.

Note also that the solution does not depend on  $q$  for both maximal and minimal input rates ( $p = 1$  and  $p = 0$ , respectively) since in these degenerate cases, all bins in all spike trains have identical values (either 1 or 0). Formally, the variances in the denominator of the Pearson coefficient, equation A.5, vanish, and the Pearson coefficient is not defined.

We noted that the output of the coincidence detector asymptotically approaches some finite value for increasing input frequencies, as can be seen in Figure 1b. We can derive a useful approximation for this asymptotic value based on equation 3.8. Setting  $p = 1$ , it is easy to show that equation 3.8 reduces to the following approximation for  $P_{out}(p = 1, q, m, \theta, U_{se}, \tau_d)$ , the asymptotic value of the output rate:

$$P_{out}(p = 1, q, m, \theta, U_{se}, \tau_d) = \sum_{k=\theta}^m \binom{m}{k} \gamma_0^k (1 - \gamma_0)^{m-k}. \quad (4.4)$$

For our simple case ( $m = 2, \theta = 2$ ), equation 4.4 further reduces to  $\gamma_0^2$ , which for the example shown in Figure 1b, and using our approximation for  $\gamma_0$  in equation 4.3, is approximately 0.2, close to the value shown in Figure 1b.

**4.2 More Realistic Example.** An illustration of equations 3.5 and 3.8 for a coincidence detector receiving  $m = 100$  binomial input spike trains with a threshold  $\theta = 15$  with and without synaptic depression is shown in Figure 2.

In Figure 2a, we reproduce the output rate of a coincidence detector without depression (equation 3.5 or, equivalently, see Mikula & Niebur, 2003). For low values of cross-correlation, the output rate of the coincidence detector is sigmoidal as a function of the input rate, rapidly saturating as the input rate increases. For increasing cross-correlation, this behavior approaches more and more a linear increase with input rate, which is, of course, nothing but the solution in which each synchronous volley of incoming action potentials leads to exactly one output spike.

Of greater interest are Figures 2b through 2d for the case of a coincidence detector receiving synaptically depressed inputs, where we obtain an inverted U-shaped curve, similar qualitatively to a resonance curve, for the output rate of a coincidence detector as a function of input rate. For increasing values of  $U_{SE}$ , progressing from Figure 2b to 2d, this behavior becomes more and more pronounced, with a sharper and sharper peak at lower and lower values of  $p$ . For perfect cross-correlation ( $q = 1$ ), the linear increase

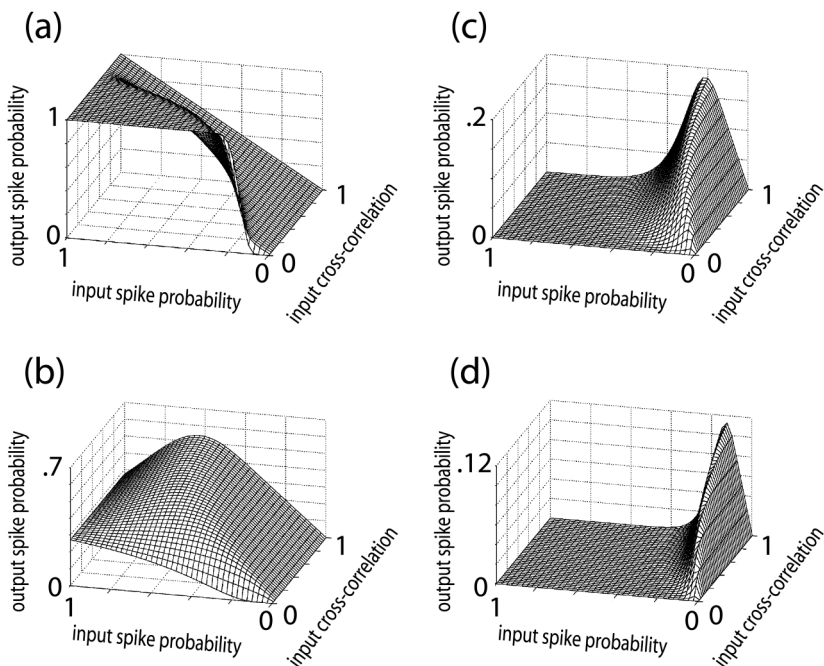


Figure 2: Analytical results for the coincidence detector. (a) Plot of equation 3.5 (no depression) for  $m = 100$  inputs and threshold of  $\theta = 15$ . (b) Plot of equation 3.8 with depression  $m = 100$  inputs,  $\theta = 15$ , and synaptic depression parameter values  $\tau_d = 700$  ms and  $U_{se} = 0.1$ . (c)  $U_{se} = 0.3$ . (d)  $U_{se} = 0.5$ .

with  $p$  (the “one spike in, one spike out” solution) always exists for low  $p$  but this regime is getting smaller and smaller, barely reaching  $p = 0.1$  in Figure 2d. As in the simple case above, approximate asymptotic values can be computed from equation 4.4.

## 5 Discussion

This article extends our previous analytical results (Mikula & Niebur, 2003) for a coincidence detector to account for probabilistic synaptic depression. The solution is for the steady-state output rate of an ideal coincidence detector receiving an arbitrary number of input spike trains with identical binomial count distributions (which includes Poisson statistics as a special case) and identical arbitrary pairwise cross-correlations, from zero correlation (independent processes) to perfect correlation (identical processes).

Activity-dependent synaptic depression is a type of neuronal response adaptation found at many synapses between cortical pyramidal cells (Thom-

son & Deuchars, 1994; Varela et al., 1997; Markram & Tsodyks, 1996; Nelson & Smetters, 1993; Finnerty et al., 1999). Although synaptic depression also exists at some synapses involving inhibitory interneurons, the predominant form of response adaptation for these connections appears to be frequency-dependent facilitation (Thomson, West, & Deuchars, 1995). Thus, the results of this article are relevant mainly for pyramidal-pyramidal connections.

The importance of synaptic depression for the decoding of temporal structures has been pointed out before. Both phasic response to a change and tonic response to a neuronal state may potentially provide important information, and both need to be understood. Abbott et al. (1997) showed that amplitude depression (depression of the amplitude of EPSPs, rather than their probabilities) allows the detection of changes in the statistics of the incoming spike trains. This article is complementary to those studies insofar as we focus here on the steady state, in the absence of transitions or transients.

Our derivation is based on a simple model. As in our previous work (Mikula & Niebur, 2003), the key assumptions of our model are as follows: (1) we do not take into account synaptic inhibition, (2) our model assumes approximately constant firing rates, (3) the model assumes probabilistic synaptic mechanisms, and (4) the bins at different times in any one of the input spike trains are independent. Of course, it should not be overlooked that a coincidence detector is a specific, memoryless model for a neuron, with a very short integration period (one time bin). This will be discussed in more detail below.

Assumption 1 means that the applicability of our model to neurons that receive strong, structured inhibitory input may be limited. The second condition implies that our results are strictly valid only for sustained input firing rates, and we make no statement for transient or changing input firing rates. The third condition means that synaptic depression operates probabilistically as opposed to the continuous modulation of EPSP amplitude depression. Our unpublished observations indicate, however, that incorporating nonprobabilistic depression does not significantly alter our results. Assumption 4 implies that our results may not be valid in the presence of significant autocorrelations in the input spike trains. We emphasize that this assumption is only about the state of time bins at different times in any one of the input spike trains. Simultaneous bins in different spike trains are not independent (their correlations are determined by  $q$ ), nor are the bins at different times in the output spike train independent (they are strongly influenced by synaptic depression).

Our results show that probabilistic synaptic depression, if made sufficiently strong and if the input is sufficiently correlated, will result in a non-monotonic, inverted U-shaped curve for the output rate of a coincidence detector as a function of input rate. In all examples shown in section 4, synaptic depression is strong enough to suppress the output frequency (probability of a spike) consistently to or below the mean input frequency if the input is

correlated. This is seen most clearly by comparing the effect with synaptic depression in Figure 2b to that without depression but otherwise identical parameters in Figure 2a. While synaptic convergence in the latter leads to a strong positive gain of the mean firing rate ( $P_{out} > p$ ; see Figure 2a) for low correlation, synaptic depression leads to an output rate that is consistently lower than the input rate ( $P_{out} < p$ ; see Figure 2b). At sufficiently high correlations, the one spike in, one spike out relationship is found again (with a gain of unity) at low firing rate, and a lower output rate (gain smaller than unity) is obtained for higher firing rates.

This result may seem counterintuitive if we consider that the probability for an EPSP event is approximately inversely proportional to the driving frequency at depressing synapses (see equation 4.3 and Abbott et al., 1997; Tsodyks & Markram, 1997). That is, for a population of incoming synapses that are presynaptically activated with a mean frequency  $f$  and whose probability of generating a postsynaptic effect is approximately  $1/f$ , the sum of the probabilities of the whole population is expected to be approximately independent of  $f$ .

While this is indeed the case for input cross-correlations of zero (see Figures 1b and 3a), where the output of the coincidence detector increases asymptotically to a constant value as input frequency is increased, it is not valid for nonzero values of input cross-correlation where a novel frequency-dependent nonmonotonic behavior emerges, becoming more prominent for higher input cross-correlations. This frequency-dependent nonmonotonic behavior runs contrary to the expectations based on the  $1/f$  approximation, though we note that for high input rates, over the input frequency range over which the output frequency becomes monotonically decreasing, the output behavior can be expected based on the qualitative arguments given at the end of section 4.

The coincidence detector is possibly the simplest neural model with any inherent time structure. To what extent do our results hold for more realistic neurons? Simulation studies (see Figure 3) indicate that our results also hold for the leaky integrate-and-fire (LIF) model (implemented such that the arrival of an input spike triggers an increase in current) with short integration time constants (less than 15 ms), in which case the LIF acts approximately like a coincidence detector.

Integration time constants of biological neurons can be on the order of 5 ms or less (due to intrinsic network activity increasing the instantaneous transmembrane conductance to a value much higher passive conductance; Destexhe & Pare, 1999; Bernander, Douglas, Martin, & Koch, 1991), and neurons in the auditory system were found to lower their time constant during development down to a few milliseconds, presumably to increase their performance as coincidence detectors (Kuba, Koyano, & Ohmori, 2002). We therefore expect that our results for the coincidence detector will have validity for more realistic neuronal models as well as for biological neurons with reasonably short integration time constants.

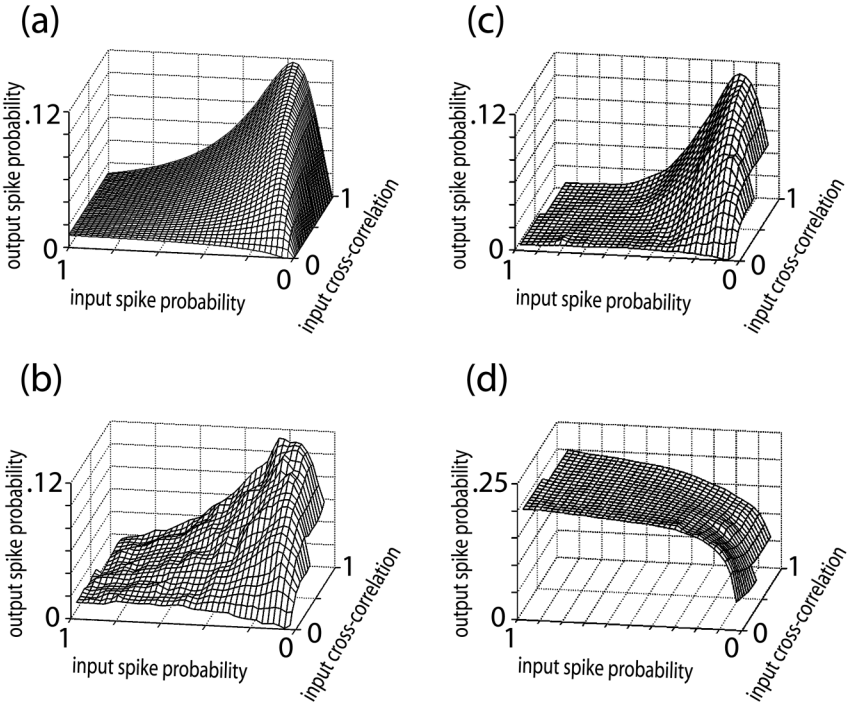


Figure 3: Comparison of analytical results for the coincidence detector (a) with simulation results for the coincidence detector (b) and a leaky integrate-and-fire neuron with short integration time constant (c) and with long integration time constant (d). Parameters are  $m = 20$ ,  $\theta = 4$ ,  $\tau_d = 700\text{ms}$ , and  $U_{se} = 0.3$ . Integration time constant for  $a$ ,  $b$ , and  $c$  is 10 ms and for  $d$  is 50 ms. In  $c$  and  $d$ , the plotted surface does not always reach the  $p = 0$  and  $p = 1$  axes because the simulations employ finite-length spike trains. Note the similarity between  $a$ ,  $b$ , and  $c$ , which indicates that our analytical results for the coincidence detector agree with simulation results for a coincidence detector and for leaky integrate-and-fire neurons with short integration time constants. However, comparing  $a$  with  $d$ , we note a marked deviation, indicating that our analytical results are valid for more realistic neuronal models only when integration time constants are short.

**Appendix: Correlation Between Pairs of Spike Trains** \_\_\_\_\_

Table 1 shows the complete probability table for all combinations of a reference spike train ( $r$ , first column) and two spike trains  $x$  and  $y$  (second and third column). The computation of the probabilities  $P_{rxy}$  (fourth column) is straightforward. For the purpose of illustration, we will compute the first three probabilities in detail here.

Table 1: Probability Table for All Combinations of the Reference Spike Train ( $r$ ) and two spike trains ( $x$  and  $y$ ) with Firing Probability  $p$  and Correlation Coefficient  $q$ .

$r$	$x$	$y$	$P_{rxy}$
0	0	0	$(1-p)[(1-p) + p\sqrt{q}]^2$
1	0	0	$p[(1-p)(1-\sqrt{q})]^2$
0	1	0	$(1-p)p(1-\sqrt{q})[(1-p) + p\sqrt{q}]$
1	1	0	$p[p + (1-p)\sqrt{q}][(1-p)(1-\sqrt{q})]$
0	0	1	$(1-p)[(1-p) + p\sqrt{q}][p(1-\sqrt{q})]$
1	0	1	$p[(1-p)(1-\sqrt{q})][p + (1-p)\sqrt{q}]$
0	1	1	$(1-p)[p(1-\sqrt{q})]^2$
1	1	1	$p[p + (1-p)\sqrt{q}]^2$

Note: In columns 1–3, 1 indicates a spike in the respective spike train and 0 stands for no spike.

In the first row,  $P_{000}$  is obtained by observing that the probability of having no spike in the reference spike train is  $(1-p)$  since the probability of obtaining a spike is  $p$ . This gives rise to the factor  $(1-p)$  in  $P_{000}$ . Given the absence of a spike in the reference spike train, there are two possibilities that spike train  $x$  also does not contain a spike in this spike train.

The first is that it starts out with no spike. This happens with the probability  $(1-p)$ , the first term in the square bracket. This is independent of the state of the reference spike train since whether a switch occurs or not, this spike train will always have no spike (switching would not change the state since, by assumption, the reference spike train does not contain a spike).

The second possibility occurs if the state in spike train  $x$  is switched to that in the reference spike train (0) even though originally (before switching) this state was 1. Since the latter occurs with the probability  $p$  and the switching with the probability  $\sqrt{q}$ , this additional probability is  $p\sqrt{q}$ , which completes the derivation of the square bracket in  $P_{000}$ . Finally, the same considerations apply to the second spike train ( $y$ ), which therefore contribute a factor equal to that obtained for  $x$  leading to the squaring of the bracket. The total probability is the product of those for the states of  $r$ ,  $x$ , and  $y$ .

The other cases in Table 1 are derived analogously. For instance,  $P_{100}$  is obtained as the product of  $p$ , which is the probability that  $r$  has a spike, and a factor of  $(1-p)(1-\sqrt{q})$  for both spike trains  $x$  and  $y$ . This latter factor is just the product of the probabilities that the spike train in question ( $x$  or  $y$ ) does not have a spike, which occurs with probability  $(1-p)$ , and that it is not switched to the state of  $r$  (given that the latter is 1), which occurs with probability  $(1-\sqrt{q})$ . Since both conditions must be met, the product of the probabilities is obtained.

The first case in Table 1 in which spike trains  $x$  and  $y$  have different states is  $r = 0, x = 1, y = 0$ , occurring with probability  $P_{010}$ . This is obtained as the product of three terms. The first is the probability of having no spike

in  $r$ , which is  $(1 - p)$ . The second is  $p(1 - \sqrt{q})$ , the probability of having a spike in  $x$  that is, furthermore, not switched to that in  $r$ . Third, the term  $[(1 - p) + p\sqrt{q}]$  reflects the two possibilities of obtaining no spike in  $y$ : either having none to begin with or having a spike that is being switched.

All the other probabilities are obtained analogously. Having obtained Table 1, it is then straightforward (although somewhat tedious) to verify the normalization condition:

$$\sum_{i=0,1} \sum_{j=0,1} \sum_{k=0,1} P_{ijk} = 1 \quad (\text{A.1})$$

Another control is to verify that the mean rate for spike train  $x$  is indeed obtained as  $p$ . Direct substitution yields

$$\langle x \rangle := \sum_{i=0,1} \sum_{k=0,1} P_{ik} = p, \quad (\text{A.2})$$

as it has to. In this equation, the first equality is the definition of the mean rate, and the second is the result of direct substitution of terms from Table 1 and straightforward (if tedious) simplification.

Clearly, we could have done the same for spike train  $y$ . More interesting is the cross-correlation. Without rate correction, it is defined as

$$\langle xy \rangle := \sum_{i=0,1} P_{i11} = (p - p^2)q + p^2, \quad (\text{A.3})$$

where the first equality defines the cross-correlation and the second is obtained after substitution from Table 1 and simplification.

It is also interesting to compute the variance of the spike trains. For instance, for spike train  $x$ , we obtain,

$$\begin{aligned} \text{var}_x &:= \langle (x - \langle x \rangle)^2 \rangle \\ &= (1 - p)^2 \sum_{i=0,1} \sum_{k=0,1} P_{ik} + p^2 \sum_{i=0,1} \sum_{k=0,1} P_{i0k} = p - p^2, \end{aligned} \quad (\text{A.4})$$

where, again, the first equality is the definition of the variance, the second results from the definition of the mean and uses equation A.2 for  $\langle x \rangle$ , and the last is the result of substitution and simplification. It is clear that the variance for spike train  $y$  has to be the same. Using equations A.3 and A.4, we can now compute the Pearson correlation coefficient of spike trains  $x$  and  $y$ :

$$\frac{\langle xy \rangle - \langle x \rangle \langle y \rangle}{\sqrt{\text{var}_x} \sqrt{\text{var}_y}} = \frac{[(p - p^2)q + p^2] - p^2}{p - p^2} = q \quad (\text{A.5})$$

We have thus verified that the correlation coefficient  $q$  introduced in our constructive method of the description of correlated spike trains is just the Pearson correlation coefficient.

## Acknowledgments

---

The material is based upon work supported by the National Science Foundation under grant number 9876271 to E.N.

## References

---

- Abbott, L. F., Varela, J. A., Sen, K., & Nelson, S. B. (1997). Synaptic depression and cortical gain control, *Science*, 275, 220–224.
- Alonso, J. M., Usrey, W. M., & Reid, R. C. (1996). Precisely correlated firing in cells of the lateral geniculate nucleus. *Nature*, 383(6603), 815–819.
- Arancio, O., Korn, H., Gulyas, A., Freund, T., & Miles, R. (1994). Excitatory synaptic connections onto rat hippocampal inhibitory cells may involve a single transmitter release site. *J. Physiol.*, 481, 395–405.
- Auger, C., Kondo, S., & Marty, A. (1998). Multivesicular release at single functional synaptic sites in cerebellar stellate and basket cells. *J. Neurosci.*, 18, 4532–4547.
- Auger, C., & Marty, A. (1997). Heterogeneity of functional synaptic parameters among single release sites. *Neuron*, 19(1), 139–150.
- Bernander, O., Douglas, R. D., Martin, K. A. C., & Koch, C. (1991). Synaptic background activity influences spatiotemporal integration in single pyramidal cells. *Proc. Nat. Acad. Sci., USA*, 88, 11569–11573.
- Buchs, N. J., & Senn, W. (2002). Spike-based synaptic plasticity and the emergence of direction selective simple cells: Simulation results. *Journal of Computational Neuroscience*, 13(13), 167–186.
- Chance, F. S., Nelson, S. B., & Abbott, L. F. (1998). Synaptic depression and the temporal response characteristics of V1 cells. *J. Neurosci.*, 18(12), 4785–4799.
- de Oliveira, S. C., Thiele, A., & Hoffmann, K. P. (1997). Synchronization of neuronal activity during stimulus expectation in a direction discrimination task. *Journal of Neuroscience*, 17(23), 9248–9260.
- Decharms, R. C., & Merzenich, M. M. (1996). Primary cortical representation of sounds by the coordination of action potential timing. *Nature*, 381, 610–613.
- Del Castillo, J., & Katz, B. (1954). Quantal components of end-plate potentials. *Journal of Physiology (London)*, 124, 560–573.
- Destexhe, A., & Pare, D. (1999). Impact of network activity on the integrative properties of neocortical pyramidal neurons in vivo. *J. Neurophysiology*, 81, 1531–1547.
- Finnerty, G., Roberts, L. S. E., & Connors, B. W. (1999). Sensory experience modifies the short-term dynamics of neocortical synapses. *Nature*, 400, 367–371.
- Fries, P., Roelfsema, P. R., Engel, A. K., König, P., & Singer, W. (1997). Synchronization of oscillatory responses in visual cortex correlates with perception in interocular rivalry. *Proc. Natl. Acad. Sci.*, 94, 12699–12704.
- Goldman, M. S., Maldonado, P., & Abbott, L. F. (2002). Redundancy reduction and sustained firing with stochastic depressing synapses. *J. Neurosci.*, 22, 584–591.

- Gray, C. M., & Viana Di Prisco, G. (1997). Stimulus-dependent neuronal oscillations and local synchronization in striate cortex of the alert cat. *J. Neurosci.*, *17*(9), 3239–3253.
- Gulyas, A. I., Miles, R., Sik, A., Toth, K., Tamamaki, N., & Freund, T. F. (1993). Hippocampal pyramidal cells excite inhibitory neurons through a single release site. *Nature*, *366*, 683–687.
- Hornoch, K., Martin, K. A. C., Jack, J. J., & Stratford, K. J. (1998). Synaptic interactions between smooth and spiny neurones in layer 4 of cat visual cortex in vitro. *J. Physiol. (Lond.)*, *508*(Pt. 2), 351–363.
- König, P., Engel, A. K., & Singer, W. (1996). Integrator or coincidence detector? The role of the cortical neuron revisited. *Trends in Neurosciences*, *719*(4), 130–137.
- Korn, H., & Faber, D. S. (1991). Quantal analysis and synaptic efficacy in the CNS. *Trends in Neurosciences*, *14*, 439–445.
- Kuba, H., Koyano, K., & Ohmori, H. (2002). Development of membrane conductance improves coincidence detection in the nucleus laminaris of the chicken. *Journal of Physiology (London)*, *540*, 529–542.
- Loebel, A., & Tsodyks, M. (2002). Computation by ensemble synchronization in recurrent networks with synaptic depression. *Journal of Computational Neuroscience*, *13*, 111–124.
- Markram, H. (1997). A network of tufted layer 5 pyramidal neurons. *Cerebral Cortex*, *7*, 523–533.
- Markram, H., & Tsodyks, M. (1996). Redistribution of synaptic efficacy between neocortical pyramidal neurons. *Nature*, *382*, 807–810.
- Matveev, V., & Wang, X. J. (2000). Implications of all-or-none synaptic transmission and short-term depression beyond vesicle depletion: A computational study. *J. Neurosci.*, *20*(4), 1575–1588.
- Mikula, S., & Niebur, E. (2003). The effects of input rate and synchrony on a coincidence detector: Analytical solution. *Neural Computation*, *15*, 539–547.
- Nelson, S. B., & Smetters, D. K. (1993). Short-term plasticity of minimal synaptic currents in visual cortical neurons. *Soc. Neurosci. Abstr.*, *19*, 629.
- Niebur, E. (2002). Electrophysiological correlates of synchronous neural activity and attention: A short review. *Biosystems*, *67*(1-3), 157–166.
- Niebur, E., Hsiao, S. S., & Johnson, K. O. (2002). Synchrony: A neuronal mechanism for attentional selection? *Current Opinion in Neurobiology*, *12*(2), 190–194.
- Niebur, E., & Koch, C. (1994). A model for the neuronal implementation of selective visual attention based on temporal correlation among neurons. *Journal of Computational Neuroscience*, *1*(1), 141–158.
- Raastad, M., Storm, J., & Andersen, P. (1992). Putative single quantum and single fibre excitatory postsynaptic currents show similar amplitude range and variability in rat hippocampal slices. *Eur. J. Neurosci.*, *4*, 113–117.
- Riehle, A., Grün, S., Diesmann, M., & Aertsen, A. (1997). Spike synchronization and rate modulation differentially involved in motor cortical function. *Science*, *278*, 1950–1953.
- Roelfsema, P. R., & Singer, W. (1998). Detecting connectedness. *Cerebral Cortex*, *8*(5), 385–396.

- Salinas, E., & Sejnowski, T. J. (2001). Correlated neuronal activity and the flow of neural information. *Nature Reviews Neuroscience*, 2(8), 539–550.
- Schikorski, T., & Stevens, C. F. (1997). Quantitative ultrastructural analysis of hippocampal excitatory synapses. *J. Neurosci.*, 17(15), 5858–5867.
- Senn, W., Segev, I., & Tsodyks, M. (1998). Reading neuronal synchrony with depressing synapses. *Neural Computation*, 10, 815–819.
- Silver, R., Cull-Candy, S., & Takahashi, T. (1996). Non-NMDA glutamate receptor occupancy and open probability at a rat cerebellar synapse with single and multiple release sites. *J. Physiol.*, 494, 231–250.
- Steinmetz, P. N., Roy, A., Fitzgerald, P., Hsiao, S. S., Johnson, K. O., & Niebur, E. (2000). Attention modulates synchronized neuronal firing in primate somatosensory cortex. *Nature*, 404, 187–190.
- Stevens, C. F., & Wang, Y. (1995). Facilitation and depression at single central synapses. *Neuron*, 14, 795–802.
- Thomson, A. M., & Deuchars, J. (1994). Temporal and spatial properties of local circuits in neocortex. *Trends in Neurosciences*, 17(3), 119–125.
- Thomson, A. M., West, D. C., & Deuchars, J. (1995). Properties of single axon excitatory postsynaptic potentials elicited in spiny interneurons by action potentials in pyramidal neurons in slice of rat neocortex. *Neuroscience*, 69(3), 727–738.
- Tong, G., & Jahr, C. E. (1994). Multivesicular release from excitatory synapses of cultured hippocampal neurons. *Neuron*, 12, 51–59.
- Tsodyks, M. V., & Markram, H. (1997). The neural code between neocortical pyramidal neurons depends on neurotransmitter release probability. *Proc. Nat. Acad. Sci., USA*, 94, 719–723. [Published erratum appears in *Proc. Natl. Acad. Sci. USA*, 94(10), 5495.]
- Varela, J. A., Sen, K., Gibson, J., Fost, J., Abbott, L. F., & Nelson, S. B. (1997). A quantitative description of short-term plasticity at excitatory synapses in layer 2/3 of rat primary visual cortex. *J. Neurosci.*, 17(20), 7926–7940.
- Walmsley, B., Alvarez, F. J., & Fyffe, R. E. (1998). Diversity of structure and function of mammalian central synapses. *Trends in Neurosciences*, 21, 81–88.